

Periodic co-continuous acoustic metamaterials with overlapping locally resonant and Bragg band gaps

Yanyu Chen and Lifeng Wang^{a)}

Department of Mechanical Engineering, State University of New York at Stony Brook, Stony Brook, New York 11794, USA

(Received 10 October 2014; accepted 4 November 2014; published online 13 November 2014)

This Letter reports a group of triply periodic co-continuous acoustic metamaterials exhibiting simultaneous wave filtering capability and enhanced mechanical properties. We numerically demonstrate the existence of complete band gaps in these acoustic metamaterials, which is attributed to the coupling effects of local resonances and Bragg scattering. Intrinsically, the coupling effects are governed by the topological arrangements of the co-continuous structures and mechanical properties of constituent phases. We further show that the frequency tunability of the complete band gaps can be achieved by tailoring the geometrical arrangements and volume fraction distribution of the co-continuous acoustic metamaterials. This work provides a clue to the design of mechanically robust acoustic metamaterials to absorb acoustic and elastic waves under harsh environments.

© 2014 AIP Publishing LLC. [<http://dx.doi.org/10.1063/1.4902129>]

In recent years, the metamaterial concept has been extended to exploit unusual mechanical properties, such as negative Poisson's ratio,^{1,2} ultra-lightweight and stiffness,³⁻⁶ high energy absorption,⁷⁻⁹ negative bulk modulus, and negative mass density.¹⁰⁻¹⁴ One particular class of mechanical metamaterials, locally resonant acoustic metamaterials, has attracted much interest because they exhibit lower frequency band gaps as compared to the Bragg band gaps in conventional phononic crystals.¹⁵⁻¹⁷ The band gaps in these acoustic metamaterials stem from local resonances associated with substructures, leading to narrow acoustic band gaps. These acoustic metamaterials offer promising applications such as wave filtering,¹⁵⁻¹⁷ acoustic cloaking,¹⁸ and energy harvesting.^{19,20} However, the substructures with local resonant units may lead to poor mechanical performance.^{21,22}

Mechanical properties such as high stiffness and high strength are essential in most structural components, yet they are often conflicting with the demand for high dissipation of wave energy induced by vibrations and shocks. Little attention, however, has been paid to the trade-off between the mechanical properties and wave filtering capability of acoustic metamaterials. This, in turn, may limit the potential employment of the metamaterials under harsh environments and extreme loading conditions. Here, we propose to introduce co-continuous acoustic metamaterials, where mechanical properties and wave energy dissipation are provided by different constituent phases. In a two-phase co-continuous composite, each constituent phase completely interpenetrates through the composite microstructure in all three dimensions and contributes its own properties in a quite independent manner to the overall properties of the composite, while these two phases are topologically interconnected and mutually reinforced in the three dimensions.^{9,23} This synergistic mechanism has been numerically and experimentally demonstrated in a group of periodic polymer co-continuous composites, which enable enhanced mechanical performance achieving a unique combination of stiffness,

strength, and energy absorption compared with other conventional composites.⁹

The model system of co-continuous metamaterials investigated here is based on level set structures possessing interfaces close to those of triply periodic minimal surfaces, and an octet-truss lattice structure (see Fig. 1). These level set structures have been shown to exhibit enhanced elastic properties compared with their rod-connected model counterparts.²⁴ While the octet-truss lattice structure is a typical stretching-dominated structure with a very high strength-to-weight ratio. It has been shown that the octet-truss lattice material can be considered as a promising alternative to metallic foams in lightweight structures.²⁵ These rationally designed periodic structures with proper combinations of constituent materials could help guide the creation of mechanically robust acoustic metamaterials.

In this letter, we combine the enhanced mechanical properties of the co-continuous metamaterials with integrated wave filtering capability resulting from the coupling effects of local resonances and Bragg scattering. We demonstrate the existence of complete band gaps in four types of metamaterials through numerical simulations. The mechanisms of the band gaps formation in the co-continuous metamaterials are discussed. Furthermore, frequency tunability of the band gaps is achieved by tailoring the topological arrangements of the co-continuous metamaterials.

Fig. 1 displays the triply periodic co-continuous metamaterials with simple cubic (SC), body-centered cubic (BCC), face-centered cubic (FCC), and octet-truss lattices, where the volume fraction (V_f) of each phase is approximately 50%. The lattice constants along three directions are all set to 2 mm. The constituent phases A and B in each metamaterial are chosen to be a ceramic (Boron Carbide, B_4C , a hard ceramic material) and a glassy polymer (SU-8, a commonly used epoxy). The material properties are characterized by Young's modulus $E_A = 460$ GPa, Poisson's ratio $\nu_A = 0.17$, and density $\rho_A = 2500$ kg/m³ for B_4C ; the ones for SU-8 are $E_B = 3.3$ GPa, Poisson's ratio $\nu_B = 0.33$ and density $\rho_B = 1180$ kg/m³. The mechanical stiffness and strength of

^{a)} Author to whom correspondence should be addressed. Electronic mail: Lifeng.wang@stonybrook.edu. Phone: 631-632-1182.

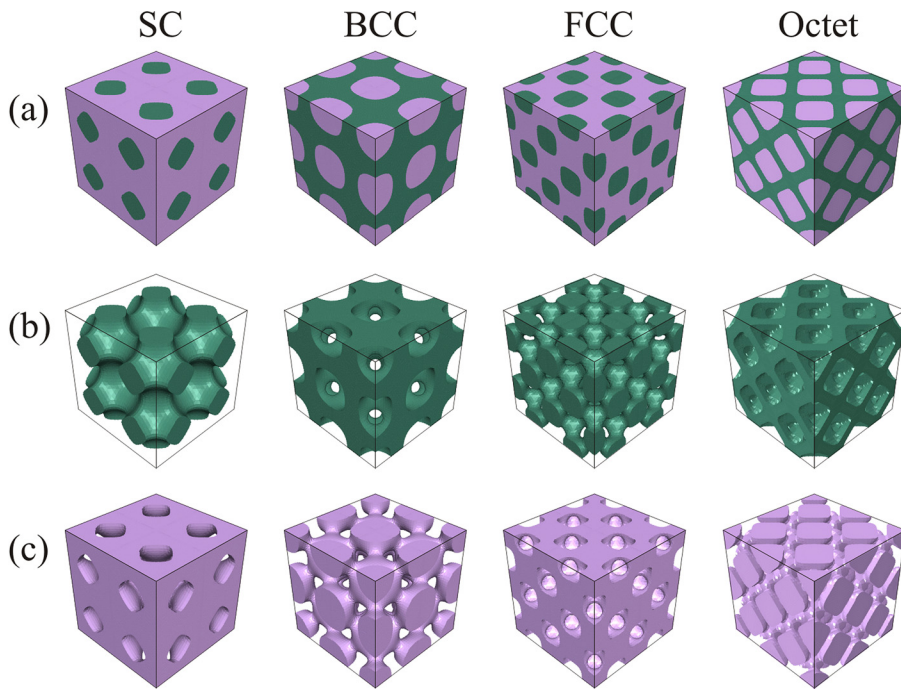


FIG. 1. (a) Triply periodic co-continuous acoustic metamaterials consisting of $2 \times 2 \times 2$ unit cells with simple cubic lattice, body-centered cubic lattice, face-centered cubic lattice, and octet-truss lattice. (b) The corresponding phase A in these metamaterials. (c) The corresponding phase B in these metamaterials. Phases A and B are separated by intermaterial dividing level set surfaces.²⁴ Reproduced by permission from Wang *et al.*, *Adv. Mater.* **23**, 1524 (2011). Copyright 2011 Wiley-VCH Verlag GmbH & Co. KGaA.

these ceramic/polymer co-continuous metamaterials are well retained due to the mutual constraints in the interpenetrating phases.⁷⁻⁹ Simply put, the band structures of the metamaterials are calculated by the finite element method (FEM) from the three dimensional (3D) elastic Lamé system. In addition, the periodic Bloch-wave boundary conditions are applied at the surfaces of the unit cell along three directions.²⁶ The transmission spectra are obtained by performing frequency domain analyses on the metamaterials consisting of finite unit cells.²⁷

The simulated band structures of the ceramic/polymer co-continuous metamaterials with SC ($V_f=59\%$), BCC ($V_f=59\%$), FCC ($V_f=62\%$), and octet-truss lattices ($V_f=49\%$)

are shown in Fig. 2. At the given volume fraction, complete band gaps arise in the band structures of the co-continuous metamaterials. To be specific, the widths of complete band gaps in the four types of metamaterials are 0.008 MHz, 0.054 MHz, 0.069 MHz, and 0.075 MHz, respectively. At the approximate volume fraction of 60%, the metamaterials with BCC and FCC lattices possess larger complete band gaps as compared to the metamaterial with SC lattice. Notably, the largest width of complete band gap is achieved in the metamaterial with octet-truss lattice at a lower volume fraction, indicating that the metamaterials with octet-truss lattice hold potential in the future design of lightweight acoustic metamaterials. It also should be noted that the frequency ranges

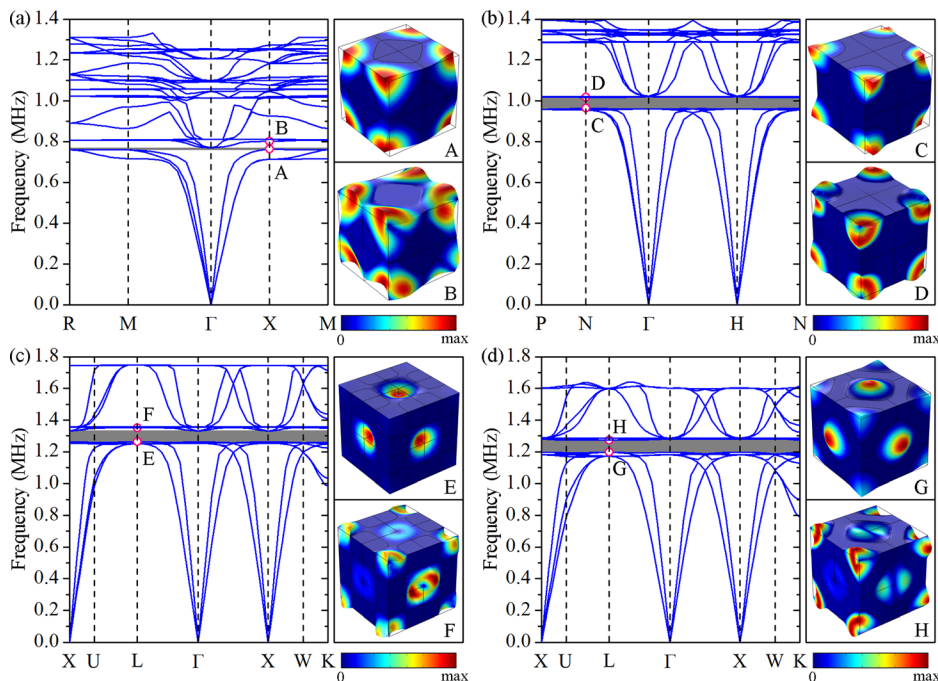


FIG. 2. Band structures and the corresponding eigenmodes of the ceramic/polymer co-continuous metamaterials with (a) SC ($V_f=59\%$), (b) BCC ($V_f=59\%$), (c) FCC ($V_f=62\%$), and (d) octet-truss ($V_f=49\%$) lattices.

of the complete band gaps reported here are much higher than those of other locally resonant metamaterials.^{15,17} This is because the relatively soft phase in the co-continuous metamaterials is much stiffer than a silicon rubber that is widely used as the soft phase in locally resonant metamaterials.

The most remarkable feature in the band structures discussed above is the existence of flat bands across the edges of Brillouin zones, which is a strong evidence of local resonances arising in these four types of co-continuous metamaterials.^{15,17} To examine the origin of these flat bands, we plot the eigenmodes on both the lower and upper edges of the band gaps, as shown in Fig. 2. Clearly, the displacements are almost localized in the relatively soft phase, indicating that the complete band gaps in the four types of co-continuous metamaterials are caused by local resonances. However, previous studies have shown that complete band gaps resulting from local resonances and Bragg scattering can coexist in periodic composites.^{28,29} To further reveal the mechanisms of complete band gaps formation, we compare the wavelength at the midgap frequency with the lattice constant of the metamaterial with FCC lattice, as an example. The wavelength at midgap frequency is given by $\lambda = c_t/\varpi$, where λ is the wavelength, c_t is the transverse velocity in the metamaterial, and ϖ is the midgap frequency. The transverse velocity in the metamaterial is given by $c_t = \sqrt{\mu^*/\rho^*}$, where μ^* and ρ^* are the effective shear modulus and effective density of the metamaterial, respectively. As a rough estimation, using the effective shear modulus (81.6 GPa) of the metamaterial calculated from FEM, we have obtained the estimated wavelength $\lambda = 5.0$ mm, half of which is the same magnitude as the lattice constant 2.0 mm. This comparison indicates that Bragg scattering also contributes to the complete band gap formation. In other words, the frequency ranges of Bragg band gaps have the same order of magnitude as those of locally resonant band gaps. Therefore, the simulated complete band gaps originate from the overlap between locally resonant band gap and Bragg band gap.

It should be pointed out that the overlapping complete band gaps reported here are different from those achieved by manipulating the periodicity of substructures in the composite media.³⁰ The coupling effects of local resonances and Bragg scattering in this work are intrinsically governed by the topological arrangements of the co-continuous structures and the mechanical properties of the constituent phases, and hence independent of lattice constants. However, the scalability of the periodic structure is still applied and can be used to achieve lower band gap frequencies as desired. Relatively soft materials (but keeping high mechanical impedance ratio between two phases) can be chosen to further lower the band gap frequency.

Additional insight into the origin of the band gaps can be gained by observing the response of the metamaterials under incident waves with different frequencies. To this end, we investigate elastic wave propagation along GX/GH direction in the co-continuous metamaterials with finite unit cells. As shown in Figs. 3(a)–3(d), strong attenuation zone in the transmission spectrum of each co-continuous metamaterial is observed, which agrees well with the partial band gap in the corresponding band structures in Fig. 2. For simplicity, taking the co-continuous metamaterial with FCC lattice as an

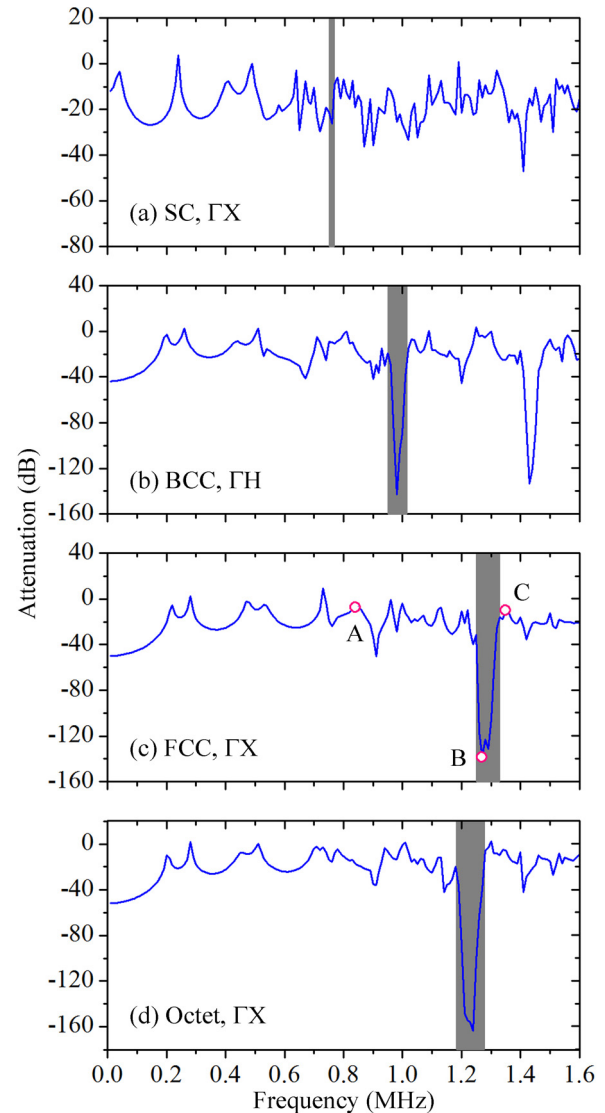


FIG. 3. Transmission spectra of the ceramic/polymer co-continuous metamaterials with (a) SC ($V_f=59\%$), (b) BCC ($V_f=59\%$), (c) FCC ($V_f=62\%$), and (d) octet-truss lattices ($V_f=49\%$) along GX/GH direction.

example, we present the response of this metamaterial under the excitation frequencies below, within and above the band gap along GX direction, respectively (Figs. 4(a)–4(c)). As expected, when the frequency of the incident wave lies below and above the band gaps, i.e., 0.85 MHz and 1.36 MHz, the incident elastic wave partially passes through and is partially reflected by the co-continuous metamaterial. In contrast, the incident elastic wave with frequency within the band gap (1.28 MHz) is localized at $x=7$ mm and its amplitude is amplified to 12.9, indicating that local resonances arise in the soft phase. The incident wave, however, attenuates rapidly after propagating for a distance of 4 mm. This phenomenon is attributed to Bragg scattering arising in the co-continuous metamaterial. The responses of the metamaterial experiencing different incident waves further support our claim that the complete band gaps result from the coupling effects of local resonances and Bragg scattering. Similar behaviors hold for other types of co-continuous metamaterials.

Acoustic metamaterials operating over narrow bandwidths are not desirable in engineering practice. To overcome

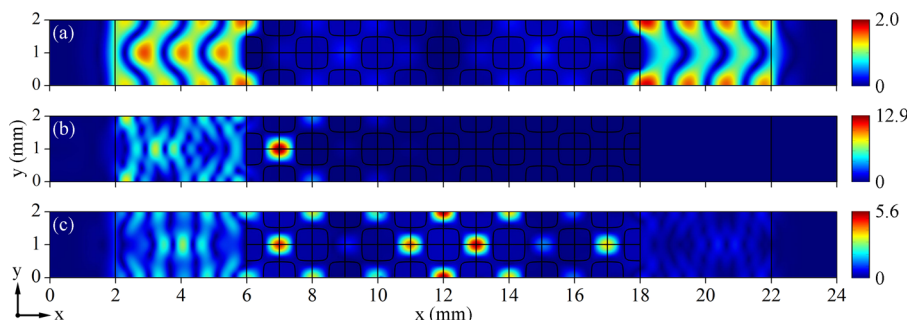


FIG. 4. Total displacement fields (μm) for excitation frequencies (a) below, 0.85 MHz; (b) within, 1.28 MHz; and (c) above, 1.36 MHz, the band gap associated with the points A, B, and C in Fig. 3(c), respectively. The incident wave with an amplitude of $1 \mu\text{m}$ is placed at $x=2 \text{ mm}$ along ΓX direction and the displacements are collected at the interface $x=22 \text{ mm}$. Periodic boundary conditions are applied at the surfaces along y and z directions. The domains within $x=[0, 2]$ and $[22, 24] \text{ mm}$ are defined as Perfectly Matched Layers.²⁷

this limitation, several approaches have been proposed to broaden the width of complete band gaps, including optimization of phononic structures,³¹ introduction of more levels of structural hierarchy,³² and use of mechanical deformation.³³ Here, we examine the effect of volume fraction of phase A on the frequency tunability in the co-continuous metamaterials. Fig. 5 plots the evolution of the complete band gaps, where for the metamaterial with SC lattice, the complete band gap opens at $V_f \approx 57\%$ and closes at $V_f \approx 60\%$, suggesting that only a small complete band gap can be achieved in a limited frequency range. While the frequency ranges of the complete band gaps in metamaterials with BCC, FCC, and octet-truss lattices are gradually increased as the volume fraction increases. Notably, the maximum widths of the complete band gaps in the metamaterials with BCC, FCC, and octet-truss lattices are 0.054 MHz, 0.079 MHz, and 0.075 MHz, respectively. These results indicate that we can achieve desired complete band gaps by tailoring topological arrangements and volume fraction of the co-continuous metamaterials.

In summary, we have presented a group of triply periodic co-continuous acoustic metamaterials with a unique combination of wave attenuation capability and enhanced mechanical properties. Unlike other pure locally resonant or Bragg band gaps, the complete band gaps reported here result from the coupling effects of local resonances and

Bragg scattering, which are intrinsically governed by the topological arrangements of the co-continuous structures and mechanical properties of constituent phases. From an engineering perspective, the localized kinetic energy resulting from local resonances could be converted into electrical energy by introducing piezoelectric materials, which could be coated on the surfaces of one phase or alternatively chosen as the soft phase. Meanwhile, the enhanced mechanical properties resulting from the synergistic mechanism of the co-continuous structures and constituent phases provide opportunities to design mechanically robust acoustic metamaterials for wave absorption under harsh environments, such as for deep water applications where high hydrostatic pressure, high dynamic load, and wave coexist. The multifunctionality in the proposed co-continuous metamaterials will be of particular interest for aerospace, automotive, and defense industries where mechanical robustness, wave filtering, and self-powering capabilities are simultaneously pursued.

This work was partially supported by the National Science Foundation under Award No. CMMI-1437449. The authors thank Professor Katia Bertoldi (Harvard University) and Professor Jiahong Sun (Chang Gung University) for valuable discussions.

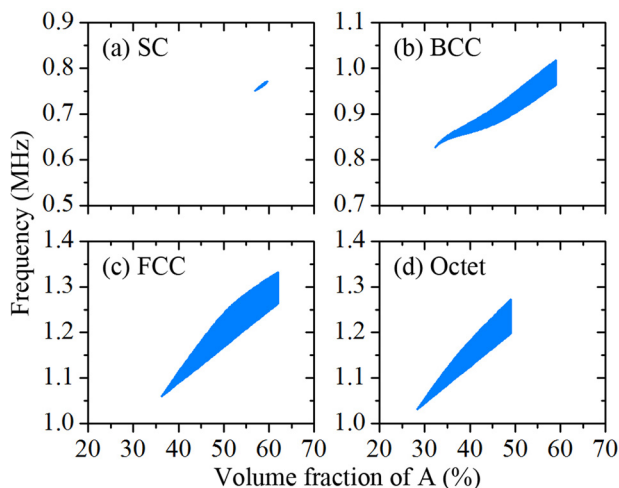


FIG. 5. Effect of volume fraction of phase A on the evolution of complete band gaps in the co-continuous acoustic metamaterials with (a) SC, (b) BCC, (c) FCC, and (d) octet-truss lattices.

¹S. Babaee, J. Shim, J. C. Weaver, E. R. Chen, N. Patel, and K. Bertoldi, *Adv. Mater.* **25**, 5044 (2013).

²X. Hou, H. Hu, and V. Silberschmidt, *Compos. Sci. Technol.* **72**, 1848 (2012).

³J. Bauer, S. Hengsbach, I. Tesari, R. Schwaiger, and O. Kraft, *Proc. Natl. Acad. Sci.* **111**, 2453 (2014).

⁴X. Zheng, H. Lee, T. H. Weisgraber, M. Shusteff, J. DeOtte, E. B. Duoss, J. D. Kuntz, M. M. Biener, Q. Ge, J. A. Jackson, S. O. Kucheyev, N. X. Fang, and C. M. Spadaccini, *Science* **344**, 1373 (2014).

⁵T. Schaedler, A. Jacobsen, A. Torrents, A. Sorensen, J. Lian, J. Greer, L. Valdevit, and W. Carter, *Science* **334**, 962 (2011).

⁶D. Jang, L. R. Meza, F. Greer, and J. R. Greer, *Nat. Mater.* **12**, 893 (2013).

⁷J.-H. Lee, L. Wang, S. Kooi, M. C. Boyce, and E. L. Thomas, *Nano Lett.* **10**, 2592 (2010).

⁸J.-H. Lee, L. Wang, M. C. Boyce, and E. L. Thomas, *Nano Lett.* **12**, 4392 (2012).

⁹L. Wang, J. Lau, E. L. Thomas, and M. C. Boyce, *Adv. Mater.* **23**, 1524 (2011).

¹⁰Y. Ding, Z. Liu, C. Qiu, and J. Shi, *Phys. Rev. Lett.* **99**, 093904 (2007).

¹¹J. Li and C. Chan, *Phys. Rev. E* **70**, 055602 (2004).

¹²Y. Cheng, J. Xu, and X. Liu, *Phys. Rev. B* **77**, 045134 (2008).

¹³X. Liu, G. Hu, G. Huang, and C. Sun, *Appl. Phys. Lett.* **98**, 251907 (2011).

- ¹⁴N. Fang, D. Xi, J. Xu, M. Ambati, W. Srituravanich, C. Sun, and X. Zhang, *Nat. Mater.* **5**, 452 (2006).
- ¹⁵Z. Liu, X. Zhang, Y. Mao, Y. Zhu, Z. Yang, C. Chan, and P. Sheng, *Science* **289**, 1734 (2000).
- ¹⁶K. M. Ho, C. K. Cheng, Z. Yang, X. Zhang, and P. Sheng, *Appl. Phys. Lett.* **83**, 5566 (2003).
- ¹⁷C. Goffaux and J. Sánchez-Dehesa, *Phys. Rev. B* **67**, 144301 (2003).
- ¹⁸S. Zhang, C. Xia, and N. Fang, *Phys. Rev. Lett.* **106**, 024301 (2011).
- ¹⁹S. Gonella, A. C. To, and W. K. Liu, *J. Mech. Phys. Solids* **57**, 621 (2009).
- ²⁰H. Lv, X. Tian, M. Y. Wang, and D. Li, *Appl. Phys. Lett.* **102**, 034103 (2013).
- ²¹H. Jiang and Y. Wang, *J. Acoust. Soc. Am.* **132**, 694 (2012).
- ²²E. Baravelli and M. Ruzzene, *J. Sound Vib.* **332**, 6562 (2013).
- ²³D. R. Clarke, *J. Am. Ceram. Soc.* **75**, 739 (1992).
- ²⁴M. Maldovan, C. K. Ullal, J. H. Jang, and E. L. Thomas, *Adv. Mater.* **19**, 3809 (2007).
- ²⁵V. S. Deshpande, N. A. Fleck, and M. F. Ashby, *J. Mech. Phys. Solids* **49**, 1747 (2001).
- ²⁶Y. Liu, X.-Z. Sun, W.-Z. Jiang, and Y. Gu, *J. Vib. Acoust.* **136**, 021016 (2014).
- ²⁷A. Khelif, Y. Achaoui, S. Benchabane, V. Laude, and B. Aoubiza, *Phys. Rev. B* **81**, 214303 (2010).
- ²⁸C. Croënne, E. Lee, H. Hu, and J. Page, *AIP Adv.* **1**, 041401 (2011).
- ²⁹Y. Chen and L. Wang, *J. Appl. Phys.* **116**, 063506 (2014).
- ³⁰N. Kaina, M. Fink, and G. Lerosey, *Sci. Rep.* **3**, 3240 (2013).
- ³¹O. Sigmund and J. S. Jensen, *Philos. Trans. R. Soc. London, Ser. A* **361**, 1001 (2003).
- ³²P. Zhang and A. C. To, *Appl. Phys. Lett.* **102**, 121910 (2013).
- ³³L. Wang and K. Bertoldi, *Int. J. Solids Struct.* **49**, 2881 (2012).